

Maxwell's Demons with Finite Size and Response Time

Nathaniel Rupprecht and Dervis Can Vural*

Department of Physics, University of Notre Dame, Notre Dame, Indiana 46556, USA

 (Received 21 March 2019; revised manuscript received 17 June 2019; published 22 August 2019)

Nearly all theoretical analyses of Maxwell's demon focus on its energetic and entropic costs of operation. Here, we focus on its rate of operation. In our model, a demon's rate limitation stems from its finite response time and gate area. We determine the rate limits of mass and energy transfer, as well as entropic reduction for four such demons: those that select particles according to (1) direction, (2) energy, (3) number, and (4) entropy. Last, we determine the optimal gate size for a demon with small, finite response time, and compare our predictions with molecular dynamics simulations with both ideal and nonideal gasses. Also, we study the conditions under which the demons are able to move both energy and particles in the chosen direction when attempting to only move one.

DOI: [10.1103/PhysRevLett.123.080603](https://doi.org/10.1103/PhysRevLett.123.080603)

Maxwell's demon is a device that can measure the microstate of a closed system, thereby reducing its entropy, seemingly in violation with the second law [1]. A century of physics literature modeling the measurement protocols and internal workings of the demon [2–5] culminated to the conclusion that logically irreversible operations taking place within the demon [6] such as information erasure [7] account for the lost entropy.

Contemporary incarnations of the demon are capable of feedback control [8,9] and universal computation [10–12]. Some demons measure and modify a tape of bits [13–16] or qubits [17] representing the state of a system, while others omit measurement altogether, instead, sorting through the microstates mechanically [18–21]. Nonideal demons have also been explored [13,14]; as have the effects of thermal equilibration of the demon with the system, and [21] studies the efficiency of an imperfect ratchet with finite mass. Today, we can build demons in the laboratory [22–33] and even make practical use of them for harvesting energy [30,34–38] or sorting atoms [39].

Experimentalists often discuss the temporal limitations of their demons, but nevertheless still operate under the simplifying assumption that the time τ it takes to sense, process, and respond to information is negligible compared to all other times [22,28,30–33]. While feedback control demons that operate periodically have been studied [33,40,41], much of their focus is on the $\tau \rightarrow 0$ or $\tau \rightarrow \infty$ limits, not on how the demon changes as τ changes, and neither treat the limitations of the demons as their main object of study.

The optimality of resetting or erasing a single bit in finite time is well understood [42–44]. In many-body context, cells constitute information engines that perform measurements and computations to process energy in a highly stochastic environment [45–49]. Here too, the timescale at which the cell operates relative

to the timescale of its environment impacts its efficiency of information processing [48].

In this Letter, we study how the transport rate attainable by a Maxwell demon operating between two chambers of gas is restricted by the finite area A of the gate that the demon controls and the rate $1/\tau$ at which the demon operates. In practice, A and τ would be constrained by experimental practicalities such as inertia and friction. Ultimately however, theoretical bounds on speed, length, and mass set the true limits on how quickly a demon can transport energy or particles. For example, the gate cannot close faster than the speed of light and must necessarily be larger than the thermal wavelength of an atom.

To this end, we study four spatiotemporally limited demons that make decisions based on direction, number, energy, or entropy measurements. For all four, we obtain heat, mass, and entropy transport as a function of τ , A . We compare our results to molecular dynamics simulations and study the conditions under which a demon is able to move both energy and particles from left to right when only aiming to move one or the other.

Problem setup.—Consider a partition separating two volumes of ideal gas, labeled as left (l) and right (r), with volumes V_l , V_r , energies E_l , E_r , and numbers of particles N_l , N_r .

In the partition between the volumes is a gate of area A , which the demon has control over. Except for the possibility of particles passing through the gate when it is open, the partitions are isolated from one another.

We also assume that each partition is large enough that it is a self-averaging canonical distribution. In this case, the speed distribution for a particle is

$$p(v) = \Omega_d v^{d-1} e^{-\beta_s m v^2/2} / Z_s, \quad Z_s = [2\pi / (m\beta_s)]^{d/2},$$

where $\Omega_d = 2, 2\pi, 4\pi$ is the solid angle in $d = 1, 2, 3$ dimensions and m is the particle mass. The index $s \in \{l, r\}$

represents a generic side. The temperature $1/\beta_s$ and energy per particle $\bar{E}_s = E_s/N_s$ are related by $\beta_s E_s = N_s d/2 \equiv \beta_s N_s \bar{E}_s$, by the equipartition theorem.

We assume that the demon decides on the state of the gate every τ seconds, which models all delays, e.g., due to measurement, processing, or physical response. We assume that after every τ , the state of the gate is updated instantaneously. Since we are interested in determining how the physical limitations of the demon restrict its ability to operate separately from information theoretical restrictions, we are not concerned with how the demon acquires information, nor how it computes its decisions.

Let \hat{A} be the event that a particle arrives at the gate within a duration of τ (i.e., passing through it if it is open, or bouncing off it if it is closed). For a randomly chosen particle with given speed v , the probability of \hat{A} is $p(\hat{A}|v) = c_d v \tau A/V$, where $c_d = 1/2, 1/\pi, 1/4$ in $d = 1, 2, 3$ dimensions (we define $A \equiv 1$ for $d = 1$). Thus, the probability that a random particle on side s impinges upon the gate during the time window is

$$p(\hat{A}) = \int_0^\infty p(\hat{A}|v) p(v) \mathbf{d}v = \kappa_s / N_s \quad (1)$$

$$\kappa_s = \frac{\rho_s \tau A}{\sqrt{2\pi\beta_s m}} = \rho_s \tau A \sqrt{\frac{\bar{E}_s}{d\pi m}} \equiv \nu_s \tau. \quad (2)$$

We will be interested in the thermodynamic limit, $N_s, V_s, E_s \rightarrow \infty$ keeping $\bar{E}_s \equiv E_s/N_s$ and $\rho_s \equiv N_s/V_s$ constant [50].

Knowing the probability that a random particle with a specific velocity arrives at the gate allows us to compute the probability that exactly n particles carrying total energy E arrives at the gate during within a duration τ ,

$$p(E, n) = \frac{\kappa_s^n (\beta_s E)^{nD}}{\Gamma(nD) n!} \frac{e^{-\beta_s E - \kappa_s}}{E}, \quad (3)$$

which can be marginalized over number or energy to find the probability of number and the probability of energy,

$$p(n|n > 0) = \frac{\kappa^n}{n!} e^{-\kappa}, \quad p(n=0) = e^{-\kappa} \delta(E) \quad (4)$$

$$p(E) = \frac{1}{E} e^{-\beta E - \kappa} \sum_{n=1}^{\infty} \frac{\kappa^n (\beta E)^{nD}}{n! \Gamma(nD)}, \quad (5)$$

where $D = (d+1)/2$. See [50] for more details of the derivation. The incomplete energy moments can be found in terms of incomplete gamma functions, $\Gamma(\cdot, \cdot)$,

$$\langle E^s \rangle_{\geq E_0} = \int_{E_0}^{\infty} E^s p(E) = \frac{e^{-\kappa}}{\beta^s} \sum_{n=1}^{\infty} \frac{\kappa^n \Gamma(nD + s, \beta E_0)}{n! \Gamma(nD)}.$$

For complete energy moments, the incomplete gamma function is replaced with a gamma function. For $s = 1$, we get the average $\langle E \rangle = \kappa D / \beta$. The number distribution moments can be found similarly, $\langle n^s \rangle = e^{-\kappa} (\kappa \partial_\kappa)^s e^\kappa$.

Entropy reduction by a demon.—Differentiating the Sackur-Tetrode equation with respect to time, we can find the entropy rates of the subsystems in terms of \dot{N}, \dot{E} . Adding the entropy rates for the two subsystems, and using mass and energy conservation, $\dot{N}_l = -\dot{N}_r, \dot{E}_l = -\dot{E}_r$, we find that the change in entropy of the whole system is

$$\frac{\dot{S}_{\text{tot}}}{k_B} = (\beta_r - \beta_l) P_\tau + \left[\frac{d}{2} \log \left(\frac{\beta_l}{\beta_r} \right) - \log \frac{\rho_r}{\rho_l} \right] I_\tau, \quad (6)$$

where I_τ and P_τ are the number and energy currents. Note that the same answer is obtained when differentiating the purely classical Clausius entropy [50].

Demon models.—We model four demons who make decisions based on direction, energy, number, and entropy. Our convention will be that each demon will attempt to move its target quantity, e.g., mass, heat, from the left partition to the right partition. For all four demons, we calculate heat P_τ , number I_τ , and entropy J_τ currents as a function of the gate area and response time, and compare these with Monte Carlo simulations (Fig. 1). We assume that even though the demon is operating, the two volumes each remain in equilibrium.

(1) A direction demon opens the gate only if there are no particles moving from right to left. Since the probability that no particles approach from the right is $e^{-\kappa_r}$, the average energy approaching the gate from the left is $D\kappa_l/\beta_l$, and the average number approaching the gate from the left is κ_l , the average heat and mass currents are

$$P_\tau^{(d)} = D\nu_l e^{-\kappa_r} / \beta_l, \quad I_\tau^{(d)} = \nu_l e^{-\kappa_r}. \quad (7)$$

Thus, the performance of the demon falls exponentially with τ . For an infinitely precise demon that can process all incoming particles ($\tau \rightarrow 0$), the rate of heat transfer is $P_0^{(s)} = (2\bar{E}_l \rho_l DA) \sqrt{\bar{E}_l / (d^3 \pi m)}$. Naturally, this only depends on the left subsystem, since the demon can shut out the right subsystem completely.

Interestingly, there is an optimal value for the area of the gate. Optimizing A for fixed τ and other system parameters shows that $A^* = (\tau \rho_r)^{-1} \sqrt{d\pi m / \bar{E}_r}$ maximizes both mass and heat transport, for $d > 1$.

(2) An energy demon opens the gate whenever the right moving particles have greater energy than left moving ones. The energy demon's heat and mass transport rate converges to that of the direction demon as $\kappa \rightarrow 0$, since the probability that multiple particles approach the gate from the right and left simultaneously vanishes. Therefore, we can write the energy demon's heat and mass currents as the direction demon's, plus correction terms [50].

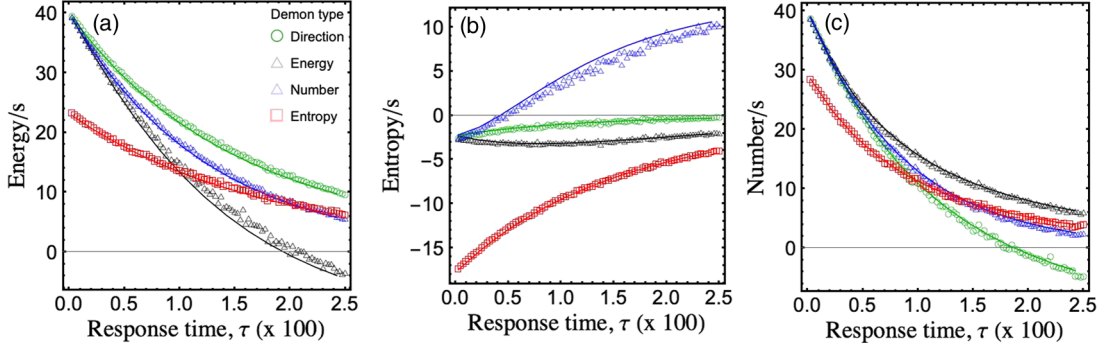


FIG. 1. Demon heat and mass transfer rates. Two different one-dimensional systems, with heat and mass currents plotted as functions of the demon's temporal resolution τ . Theory (solid lines) agrees with simulations (dots). (a) The subsystems have a temperature difference, but with the same number density, $\beta_l = 1$, $\beta_r = 0.25$, $\rho_l = \rho_r = 100$. Note that the heat transfer rate can be negative for the number demon. (b) The change in system entropy per unit time for the same system as in the left panel. (c) The right subsystem has a lower temperature and a much higher number density than the left subsystem, $\rho_l = 100$, $\rho_r = 400$, $\beta_l = 1$, $\beta_r = 2$. Here, it can be seen that the energy demon has a negative number current for large τ .

$$P_\tau^{(e)} = P_\tau^{(d)} + \frac{\nu_l \nu_r \Gamma(2D+1)}{\Gamma(D)^2} (-1)^D \left(\frac{f_1}{\beta_l} + \frac{f_2}{\beta_r} \right) \tau e^{-\kappa_l - \kappa_r}$$

$$I_\tau^{(e)} = I_\tau^{(d)} + \frac{\Gamma(3D) \tau^2 e^{-\nu_l - \kappa_r}}{2\Gamma(2D)\Gamma(D+1)} \left(\nu_l^2 \nu_r f_3 - \frac{\nu_l \nu_r^2}{2} f_4 \right), \quad (8)$$

where $f_1 = B(-\beta_l/\beta_r, D, -2D)$ and $f_2 = B(-\beta_l/\beta_r, D+1, -2D)$ are Euler beta functions, and $f_3 = F_{2,1}(D, 3D; D+1; -\beta_r/\beta_l)$ and $f_4 = F_{2,1}(2D, 3D; 2D+1; -\beta_l/\beta_r)$ are hypergeometric functions.

It is not difficult to numerically solve for $P_\tau^{(e)}$, $I_\tau^{(e)}$ for higher dimensions. An exact analytical solution for heat and mass transport for $d = 1$ is given in [50].

(3) A number demon opens the gate if right-moving particles are more than left-moving ones. An exact solution for $d = 1$ is again [50], for $d > 1$, we again obtain the leading order correction,

$$P_\tau^{(n)} = P_\tau^{(d)} + \frac{\nu_l^2 \nu_r}{2\beta_l} \tau^2 (d+2) \left(1 - \frac{1}{2} \frac{d+3\beta_l}{d+2\beta_r} \right) e^{-\kappa_l - \kappa_r}$$

$$I_\tau^{(n)} = I_\tau^{(d)} + \frac{\nu_l^2 \nu_r}{2} \tau^2 e^{-\kappa_l - \kappa_r}. \quad (9)$$

(4) An entropy demon opens the gate if doing so reduces the total entropy, i.e., if

$$E_r - E_l > \left[\log \frac{\rho_r}{\rho_l} - \frac{d}{2} \log \left(\frac{\beta_l}{\beta_r} \right) \right] \frac{n_l - n_r}{\beta_l - \beta_r} \equiv \chi(n_l - n_r).$$

If $\beta_l = \beta_r$, the entropy demon opens the gate whenever $n_l > n_r$, acting as a number demon, and if $\chi = 0$, it acts as an energy demon. The average heat and mass flow is

$$J = \sum_{n_l, n_r=0}^{\infty} \int_0^{\infty} \mathbf{d}E_l \mathbf{d}E_r p_{n_l}^{(l)}(E_l) p_{n_r}^{(r)}(E_r) j(\{E_s\}, \{n_s\})$$

$$j(\{E_s\}, \{n_s\}) = \Theta[E_r - E_l - \chi(n_l - n_r)] \Delta(\{E_s\}, \{n_s\}),$$

with a step function enforcing the inequality above. Here, $\Delta = E_l - E_r$ for $J = P_\tau$ and $\Delta = n_l - n_r$ for $J = I_\tau$.

The entropy demon behaves different than the number and energy demons; it does not act as a direction demon as $\tau \rightarrow 0$.

Simulations.—We distribute particles uniformly in space, assign them Boltzmann-distributed velocities, and obtain the time they approach the gate and the energy they carry. For $d > 1$, the probability of atoms arriving the gate decreases with decreasing gate area. Thus, for economical reasons, we run most simulations only for $d = 1$. In all plots, the units of temperature are such that $k_B = 1$. See [50] for simulation details.

In Fig. 1, we compare the energy, mass, and entropy currents generated by the demons to our formulas. In panels (a),(b), the right chamber has a temperature four times greater than the left, and the number densities are the same. In panel (c), the temperatures of the right chamber are half of that of the left, but the number density of the right chamber is four times that of the left.

Figure 1 illustrates an interesting phenomenon. For demons with fast response time (i.e., small τ), regardless of whether they are aiming to transport heat or mass, they end up transporting both quantities in the same direction. However, at sufficiently large τ (and, as we will see, large enough values of ρ_r or T_r), heat and mass transport can be in opposite directions. For example, the number demon is willing to let a few very energetic molecules move from right to left as long as a larger number of less energetic molecules move from left to right. We define τ_c to be the response time for which demons start pumping particles or energy from right to left instead of left to right.

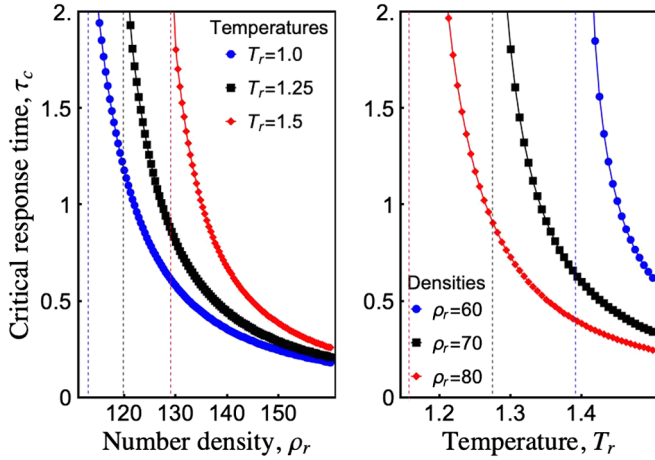


FIG. 2. Critical response time. The critical τ for energy and number demons, along with estimates of the critical values below which no τ_c exists. Above τ_c , the demon will transfer heat or mass from right to left instead of from left to right. In both plots, the left subsystem has $T_l = 1$, $\rho_l = 100$, only the parameters of the right subsystem are varied. Left: the energy demon's τ_c for different right subsystem temperatures, varying right subsystem number density. Right: the number demon's τ_c , for different right subsystem number densities, varying the right subsystem's temperature.

Figure 2 illustrates the behavior of τ_c . Theoretical values of τ_c are plotted, varying either number density (for the energy demon, left) or temperature (for the number demon, right).

For low enough number density or temperature, there may not be a τ_c (it diverges at some critical number density or temperature). For $\tau < \tau_c$, either demon strategy is appropriate for ensuring that there is no “backwash” of particles or energy from right to left, while above τ_c , a specific strategy must be favored to ensure this. This illustrates another difference between our demons and ideal demons. An ideal, infinitely quick demon does not have to prioritize particle number or energy no matter what the number densities or temperatures of the subsystems are, but a restricted demon has to consider tradeoffs.

To check the generality of our prediction, we also ran molecular dynamics simulations of demons operating in two dimensions with ideal and hard sphere gasses, the results of which can be seen in Fig. 3. Because of computational constraints, the data are more noisy than the one-dimensional case, but clearly the prediction and theory match well for ideal gas demons. Although our equations are only valid for ideal gasses, the currents for demons working with hard sphere gasses have qualitatively similar decaying behavior as the predictions. For example, $P^{(e)}$ and $P^{(n)}$ are overestimated, and $N^{(e)}$ is underestimated by the predictions, but all curves are qualitatively similar. We have also observed that the hard sphere demon's rates approach the corresponding ideal demon's rates as we reduce the volume of each individual particle. A video showing an energy demon in operation can be seen in the

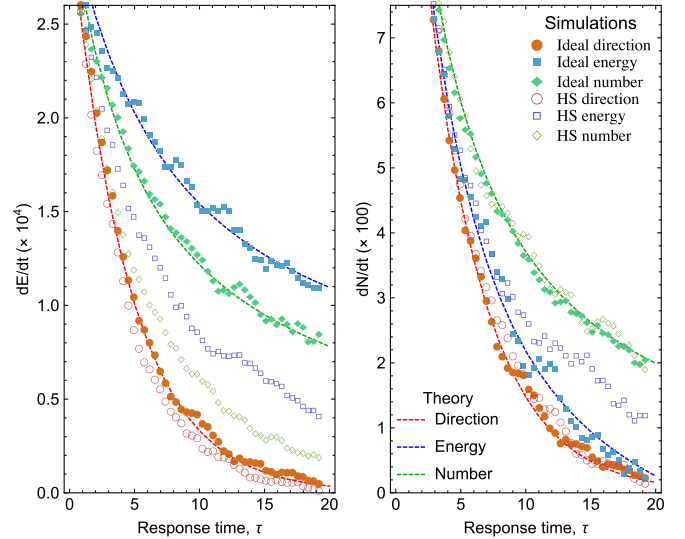


FIG. 3. Two-dimensional demon. A two-dimensional Maxwell demon, operating on an ideal gas and a hard sphere gas. The energy (left) and number (right) rate of demons working with an ideal gas match well with prediction for all three demon types, and the hard sphere gas is qualitatively similar. The system has $\rho_l = 1.5$, $\rho_r = 3$, and $T_l = 0.0015$, $T_r = 0.001$. The dimensions of each subsystem are 30×30 , and the particle radius is 0.025. The packing fraction of the left and right subsystems are $\phi_l = 0.0029$, $\phi_r = 0.0059$.

Supplemental Material, which also has more simulation details [50].

Discussion.—Most literature on the Maxwell's demon focuses on its thermodynamic cost of operation. Here we point out that even if a demon has no restrictions on memory, or knowledge of the state of the systems, it will still be limited in its rate of operation due to its physical characteristics. Here, we determined rate bounds for four kinds of demons. We have derived the optimal area of the gate for the simple demon, and by extension, for all demons with small τ , and how the demons' response time and gate size determine heat, mass, and entropy currents.

For a square gate with $A = 1 \mu\text{m}^2$ that moves at the speed of light to sort air molecules at 300 K and standard pressure, we get $\kappa \sim 9.5$. For a simple demon, the energy and number transfer for a demon with $\tau > 0$ is $e^{-\kappa\tau}$ times less than a demon operating with $\tau = 0$, meaning that its currents would be $\sim 7.5 \times 10^{-5}$ times less than an infinitely fast demon.

Of course, not all realizations of Maxwell's demons operate via gates. For example, many nanomolecular pumps and refrigerators are implemented by single electron transistors. However, these devices still have spatial and temporal restrictions that play similar roles, such as finite sampling and feedback rates, the probability rate of electron tunneling and cotunneling events, and quantum confinement effects [31,51,52]. As such devices become widespread, it will be crucial to know how their spatial and temporal limitations influence transport rates.

*Corresponding author.
dvural@nd.edu

- [1] J. C. Maxwell, *Theory of Heat* (Longmans, Green, 1891).
- [2] W. Thomson, *Nature (London)* **9**, 232 (1874).
- [3] M. Smoluchowski, *Pisma Mariana Smoluchowskiego* **2**, 226 (1927).
- [4] L. Szilard, *J. Phys.* **53**, 840 (1929).
- [5] L. Brillouin, *J. Appl. Phys.* **22**, 334 (1951).
- [6] C. H. Bennett, *Int. J. Theor. Phys.* **21**, 905 (1982).
- [7] R. Landauer, *IBM J. Res. Dev.* **5**, 183 (1961).
- [8] F. J. Cao, L. Dinis, and J. M. R. Parrondo, *Phys. Rev. Lett.* **93**, 040603 (2004).
- [9] U. Seifert, *Rep. Prog. Phys.* **75**, 126001 (2012).
- [10] W. Zurek, *Algorithmic Randomness, Physical Entropy, Measurements, and the Demon of Choice* (Perseus Books, Reading, 1999).
- [11] C. M. Caves, *Phys. Rev. Lett.* **64**, 2111 (1990).
- [12] C. M. Caves, W. G. Unruh, and W. H. Zurek, *Phys. Rev. Lett.* **65**, 1387 (1990).
- [13] D. Mandal and C. Jarzynski, *Proc. Natl. Acad. Sci. U.S.A.* **109**, 11641 (2012).
- [14] D. Mandal, H. T. Quan, and C. Jarzynski, *Phys. Rev. Lett.* **111**, 030602 (2013).
- [15] A. C. Barato and U. Seifert, *Europhys. Lett.* **101**, 60001 (2013).
- [16] A. Hosoya, K. Maruyama, and Y. Shikano, *Sci. Rep.* **5**, 17011 (2015).
- [17] S. Deffner, *Phys. Rev. E* **88**, 062128 (2013).
- [18] R. P. Feynman, R. B. Leighton, and M. Sands, *The Feynman Lectures on Physics, Vol. I: The New Millennium Edition: Mainly Mechanics, Radiation, and Heat* (Basic Books, New York, 2011), Vol. 1.
- [19] L. Gordon, *Found. Phys.* **13**, 989 (1983).
- [20] P. A. Skordos and W. H. Zurek, *Am. J. Phys.* **60**, 876 (1992).
- [21] Z. Tu, *J. Phys. A* **41**, 312003 (2008).
- [22] P. Strasberg, G. Schaller, T. Brandes, and M. Esposito, *Phys. Rev. Lett.* **110**, 040601 (2013).
- [23] É. Roldán, I. A. Martínez, J. M. Parrondo, and D. Petrov, *Nat. Phys.* **10**, 457 (2014).
- [24] N. Cottet, S. Jezouin, L. Bretheau, P. Campagne-Ibarcq, Q. Ficheux, J. Anders, A. Auffèves, R. Azouit, P. Rouchon, and B. Huard, *Proc. Natl. Acad. Sci. U.S.A.* **114**, 7561 (2017).
- [25] J. J. Thorn, E. A. Schoene, T. Li, and D. A. Steck, *Phys. Rev. Lett.* **100**, 240407 (2008).
- [26] S. T. Bannerman, G. N. Price, K. Viering, and M. G. Raizen, *New J. Phys.* **11**, 063044 (2009).
- [27] J. V. Koski, A. Kutvonen, I. M. Khaymovich, T. Ala-Nissila, and J. P. Pekola, *Phys. Rev. Lett.* **115**, 260602 (2015).
- [28] M. D. Vidrighin, O. Dahlsten, M. Barbieri, M. S. Kim, V. Vedral, and I. A. Walmsley, *Phys. Rev. Lett.* **116**, 050401 (2016).
- [29] P. A. Camati, J. P. S. Peterson, T. B. Batalhao, K. Micadei, A. M. Souza, R. S. Sarthour, I. S. Oliveira, and R. M. Serra, *Phys. Rev. Lett.* **117**, 240502 (2016).
- [30] K. Chida, S. Desai, K. Nishiguchi, and A. Fujiwara, *Nat. Commun.* **8**, 15310 (2017).
- [31] G. Schaller, C. Emary, G. Kiesslich, and T. Brandes, *Phys. Rev. B* **84**, 085418 (2011).
- [32] M. Esposito and G. Schaller, *Europhys. Lett.* **99**, 30003 (2012).
- [33] G. Schaller, J. Cerrillo, G. Engelhardt, and P. Strasberg, *Phys. Rev. B* **97**, 195104 (2018).
- [34] L. Gammaitoni, *Contemp. Phys.* **53**, 119 (2012).
- [35] S. Bo, M. Del Giudice, and A. Celani, *J. Stat. Mech.* (2015) P01014.
- [36] B. Sothmann, R. Sánchez, and A. N. Jordan, *Nanotechnology* **26**, 032001 (2015).
- [37] B. Roche, P. Roulleau, T. Jullien, Y. Jompol, I. Farrer, D. A. Ritchie, and D. Glatli, *Nat. Commun.* **6**, 6738 (2015).
- [38] F. Hartmann, P. Pfeffer, S. Höfling, M. Kamp, and L. Worschech, *Phys. Rev. Lett.* **114**, 146805 (2015).
- [39] M. G. Raizen, *Sci. Am.* **304**, 54 (2011).
- [40] G. Engelhardt and G. Schaller, *New J. Phys.* **20**, 023011 (2018).
- [41] J. Bergli, Y. M. Galperin, and N. B. Kopnin, *Phys. Rev. E* **88**, 062139 (2013).
- [42] A. Béruit, A. Arakelyan, A. Petrosyan, S. Ciliberto, R. Dillenschneider, and E. Lutz, *Nature (London)* **483**, 187 (2012).
- [43] C. Browne, A. J. P. Garner, O. C. O. Dahlsten, and V. Vedral, *Phys. Rev. Lett.* **113**, 100603 (2014).
- [44] P. R. Zulkowski and M. R. DeWeese, *Phys. Rev. E* **89**, 052140 (2014).
- [45] P. Mehta and D. J. Schwab, *Proc. Natl. Acad. Sci. U.S.A.* **109**, 17978 (2012).
- [46] A. C. Barato, D. Hartich, and U. Seifert, *Phys. Rev. E* **87**, 042104 (2013).
- [47] A. H. Lang, C. K. Fisher, T. Mora, and P. Mehta, *Phys. Rev. Lett.* **113**, 148103 (2014).
- [48] A. C. Barato, D. Hartich, and U. Seifert, *New J. Phys.* **16**, 103024 (2014).
- [49] P. Sartori, L. Granger, C. F. Lee, and J. M. Horowitz, *PLoS Comput. Biol.* **10**, e1003974 (2014).
- [50] See Supplemental Material at <http://link.aps.org/supplemental/10.1103/PhysRevLett.123.080603>, Sec. A for estimates on the error that this introduces for finite systems and expanded derivations, Sec. B for exact solutions for the one-dimensional demons, Sec. C for various integrals and identities, Sec. D for an example derivation, Sec. E for more details on demon entropy and notes on the entropic cost of operating the demons, and Sec. F for simulation details.
- [51] J. Deng and H.-S. P. Wong, *IEEE Trans. Electron Devices* **54**, 3186 (2007).
- [52] J. Deng and H.-S. P. Wong, *IEEE Trans. Electron Devices* **54**, 3195 (2007).